HHS Public Access

Author manuscript

J Immunol. Author manuscript; available in PMC 2016 April 15.

Published in final edited form as:

J Immunol. 2015 April 15; 194(8): 3840–3851. doi:10.4049/jimmunol.1402685.

Mast cells play an important role in *Chlamydia pneumoniae* lung infection by facilitating immune cell recruitment into the airway

Norika Chiba[†,§], **Kenichi Shimada**[†,§], **Shuang Chen**[†], **Heather D. Jones**[‡], **Randa Alsabeh**[¶], **Anatoly V. Slepenkin**[#], **Ellena Peterson**[#], **Timothy R. Crother**[†,*], and **Moshe Arditi**[†,*]

[†]Division of Pediatrics Infectious Diseases and Immunology and Department of Biomedical Sciences, Cedars-Sinai Medical Center (CSMC) and David Geffen School of Medicine, UCLA, Los Angeles, CA 90048, USA

[‡]Division of Pulmonary and Critical Care Medicine, Dept. of Medicine, Cedars-Sinai Medical Center (CSMC) and David Geffen School of Medicine, UCLA, Los Angeles, CA 90048, USA

[¶]Department of Pathology and Laboratory Medicine, Cedars-Sinai Medical Center (CSMC) and David Geffen School of Medicine, UCLA, Los Angeles, CA 90048, USA

[#]Department of Pathology, University of California Irvine, Irvine, CA 92697, USA

Abstract

Mast cells are known as central players in allergy and anaphylaxis, and play a pivotal role in host defense against certain pathogens. *Chlamydia pneumoniae* (Cpn) is an important human pathogen, but it is unclear what role mast cells play during Cpn infection. We infected C57BL/6 (WT) and mast cell-deficient mice, Kit$^{w\text{-}sh/w\text{-}sh}$ (Wsh), with Cpn. Wsh mice showed improved survival than WT, with fewer cells in Wsh BALF despite similar levels of cytokines and chemokines. We also found a more rapid clearance of bacteria from the lungs of Wsh mice compared with WT. Cromolyn, a mast cell stabilizer, reduced BAL cells and bacterial burden similar to Wsh mice; conversely, Compound 48/80, a mast cell degranulator, increased the number of BAL cells and bacterial burden. Histology showed that WT lungs had diffuse inflammation while Wsh mice had patchy accumulations of neutrophils and perivascular accumulations of lymphocytes. Infected Wsh mice had reduced amounts of MMP-9 in BALF and were resistant to epithelial integral membrane protein degradation, suggesting that barrier integrity remains intact in Wsh mice. Mast cell reconstitution in Wsh mice led to enhanced bacterial growth and normal epithelial integral membrane protein degradation, highlighting the specific role of mast cells in this model. These data suggest that mast cells play a detrimental role during Cpn infection by facilitating immune cell infiltration into the airspace and providing a more favorable replicative environment for Cpn.

Corresponding Author: Moshe Arditi, MD. Cedars Sinai Medical Center, Department of Biomedical Sciences, Division of Pediatric Infectious Diseases and Immunology, 8700 Beverly Blvd. Rm 4221. Los Angeles, California, 90048, USA. Phone: (310) 423-4471; Fax: (310) 423 8284; moshe.arditi@cshs.org.

[*]These authors contributed equally to the manuscript.

[§]These authors contributed equally to the manuscript.

Disclosures

None.

Keywords

mast cells; Chlamydia pneumonia; inflammation; cell recruitment; airways

Introduction

Chlamydia pneumoniae (Cpn), an obligate intracellular pathogen, is responsible for up to 10–20% community acquired pneumonia and is associated with many chronic inflammatory disorders including atherosclerosis, asthma, and Alzheimer's disease (1–6). Most people will become seropositive for Cpn, and the titer of anti-Cpn Ab increases with age, indicating continued exposure and immune response throughout life. (1–7). Thus, understanding the mechanism of Cpn-induced inflammatory responses of the host remains an important endeavor. We and other researchers have reported that Cpn is recognized by the pattern recognition receptors (PRRs) such as Toll-like receptor 2 (TLR) and TLR4, which signal through MyD88 and Trif, and the NOD-like receptors (NLRs), Nod1 and Nod2, which signal through Rip2 (8–11). More recently, we and others have shown that Cpn activates the NLRP3 inflammasome activation directly (12–14), resulting in mature IL-1β production, which is critical for proper immune responses against Cpn infection (14, 15). In the airway, Cpn infects alveolar macrophages and airway epithelial cells first, which in turn secrete proinflammatory cytokines and chemokines that results in the influx of inflammatory cells such as monocytes, macrophages, and neutrophils (10, 16, 17). One report observed that Cpn infection could induce human mast cells to produce cytokines *in vitro* and that a pulmonary Cpn infection in mice led to mast cell degranulation *in vivo* (18).

Mast cells (MCs) are best known as playing a key role in allergy, anaphylaxis, and host defense against helminth parasites by releasing chemical mediators such as histamine, leukotrienes, and mast cell proteases. Recently, it has been reported that MCs can recognize bacterial pathogens through TLRs and NLRs, produce pro-inflammatory cytokines (19–21), and play an important role in host defense against bacteria (12, 22–29). Mast cell proteases (MCPTs) such as tryptase and chymase degrade many proteins including extracellular matrix (ECM) (30, 31). In addition, chymase (MCPT4) has been reported to activate matrix metalloprotease (MMP)-9 by cleaving a specific site of the catalytic domain of MMP-9 (32–34); chymase inhibitors reduces both the pro- and active form of MMP-9 and attenuates its enzymatic activity *in vivo* (35, 36). MMP-9 is of particular interest in pulmonary infections because it is necessary for both neutrophil infiltration into the lung and airspace (35, 37) and intratracheal migration of dendritic cells (38, 39). Furthermore, MMP degrades claudins, adhesion molecules important in cell-cell tight junctions, during influenza-induced lung injury (39–41). In the lung, several claudin family members are expressed, including claudin-5 and 18, which are components of alveolar tight junctions (37, 38, 42), and their degradation is important for paracellular permeability and cell transmigration (40, 43).

In the present study, we found that mast cells were required for normal immune cell infiltration into the airspaces during a Cpn lung infection in mice. Mast cell deficiency resulted in faster bacterial clearance and reduced lung inflammation. Prevention of mast cell degranulation phenocopied mast cell deficiency while pharmacological induction of mast

cell degranulation resulted in greater inflammatory responses to Cpn infection. Mast cell deficient mice had less MMP9 secretion and activation, and less degradation of claudin 5 and 18, suggesting that mast cells are required for the opening of tight junctions to allow immune cells to infiltrate into the airspaces during a bacterial infection. Finally, mast cell reconstitution in Wsh resulted in greater bacterial growth, increased MMP9, and degradation of claudin 5. These data suggest an unappreciated role for mast cells as gatekeepers to facilitate immune cell infiltration into the airspace by regulating tight junction opening during Cpn lung infection, where immune cell infiltration into host lungs is required for normal Cpn propagation. Thus unlike most other infections where mast cells are protective, mast cells appear to play an important role in the pathogenesis of Cpn infection in mice.

Methods

Animals and Reagents

C57BL/6 (WT) and Wsh ($Kit^{W\text{-}sh/W\text{-}sh}$) mice were purchased from The Jackson Laboratory (Bar-Harbor, ME, USA). Eight to 10-week old female mice were used throughout the all experiments in this study. All experiments were done according to Cedars-Sinai Medical Center Institutional Animal Care and Use Committee guidelines. Cromolyn and Compound 48/80 were purchased from SIGMA-ALDRICH (St. Louis, MO, USA).

Cpn infection and sample preparation

C. pneumoniae CM-1 (ATCC, Menassa, VA) was propagated in HEp-2 cells as previously described (8, 44). Both HEp-2 cells and Cpn aliquot were confirmed as *Mycoplasma* free by PCR. Mice were infected with either 2 or 5×10^6 IFU Cpn by inoculating intratracheally. Bronchoalveolar Lavage Fluid (BALF) was collected by injecting 0.5 mL of PBS containing 5 mM EDTA. BALF was separated into supernatant and cells by centrifugation. Supernatant was used for cytokine and chemokine measurements and Western Blotting. Cells were smeared on glass slide, and then stained by modified Wright-Giemsa staining (Diff-Quick, Fisher Scientific, Pittsburgh, PA, USA) to determine subtypes of leukocyte by their cellular and nuclear characteristics. Lungs were homogenized with 1 mL of ice-cold sucrose-phosphate-glutamate medium for cytokine and chemokine measurements and bacterial burden quantification.

Bacterial Burden quantification

HEp-2 cells were infected with Cpn in lung specimens for bacterial burden quantification as described previously (45, 46). Briefly, HEp-2 cells were incubated with diluted lung suspensions or cell lysates in the presence of 1 ug/mL cycloheximide and 10 μg/mL gentamicin containing RPMI1640 medium. Centrifugation was done for first 1 hour at 800x g, and then cells placed in incubator (37°C, 0.5% CO_2). After 72 hours culture, cells were washed with PBS and fixed with methanol, and then stained with FITC-conjugated anti-*Chlamydia* genus-specific mAb (Pathfinder Chlamydia Culture Confirmation System, BIO-RAD, Hercules, CA, USA) according the manufactures' instruction. Cpn inclusions in cells were counted by fluorescence microscopic analysis.

Mast cell reconstitution

Bone marrow cells from C57BL/6 mice were cultured in RPMI1640 medium supplemented with 10% FBS and 20% WEHI-3 conditioned media for 6~8 weeks to differentiate to Bone marrow derived Mast cells (BMMC). BMMC were confirmed as c-kit+ FcERIa+ by flow cytometry. Six weeks old Wsh mice received tail vein injection of 5×10^6 BMMC. Twelve weeks after reconstitution, mice were sacrificed, then collected tissues and peritoneal lavages, and accessed for reconstitution of mast cell deficiency.

Flow cytometry analysis

Lungs were digested enzymatically to isolate leukocytes in the tissue for flow cytometric analysis as previously described (17, 47). Briefly, lungs were digested at 37°C for 20 minutes in HANKS buffer containing 40 units/mL Liberase (Roche Diagnostics, Indianapolis, IN, USA) and 50 units/mL DNase I (Roche Diagnostics). Cells were then filtered through 70 μm cell strainer (BD Biosciences, San Jose, CA, USA). Erythrocytes were obviated by RBC Lysis Buffer (eBioscience, San Diego, CA, USA). Single cells were stained with the following antibodies; F4/80 Ab, CD11c Ab, Ly6G Ab, CD11b Ab, TREM1 Ab, CD4 Ab, CD44 Ab, c-kit Ab, IgE Ab, Lamp1 Ab, and CD62L Ab. For lung single cell differentials, cell types were identified as: neutrophils CD11c- CD11b+ Ly6G+, alveolar macrophages CD11b+ CD11c+ F4/80+, T-cells CD3+ and either CD4 or CD8 positivity. Mast cells were identified as side scatter high and c-kit+ IgE+. Mast cell degranulation was evaluated by surface LAMP1 staining. For intracellular Chlamydia staining, cells were permeabilized using Cytofix/Cytoperm kit (BD Biosciences) and stained with anti-*Chlamydia* LPS mAb (Accurate Chemical and Scientific Corporation, Westbury, NY, USA) and PE-conjugate anti mouse. Flow cytometric analysis was performed using a CyAn™ flow cytometer (Beckman Coulter) and analyzed using Summit (Dako, Carpinteria, CA, USA) software.

Evaluation of vascular permeability

Mice received 25 mg/kg Evans blue dye via tail vein injection 2 h before lung harvest. Lungs were homogenized with 1 mL PBS. Centrifuged and pellets were incubated with 500 mL formamide at 60 °C for 18 hrs. The supernatant was measured at absorbencies 620 nm – 740 nm. For airway permeability, mice were injected with Evans blue dye as above, sacrificed 2hr later, and BALF was obtained. The supernatant was measured at absorbencies 620 nm – 740 nm.

Histopathological analysis

Lungs were fixed in formalin buffer and embedded in paraffin for histological analysis. Paraffin-embedded lungs were cut and stained with hematoxylin and eosin (H&E). Immunohistochemistry was performed by using anti-CD3 Ab (clone 2GV6) prediluted from Ventana Medical Systems (Yuscon, AZ, USA), anti-CD20 Ab (goat polyclonal) from Santa Cruz Biotechnologies (CA, USA), and anti-Ly6G Ab (clone 1A8) from eBioscience. Sections incubated with isotype control antibody and HRP-conjugated secondary antibody were used as negative controls. Staining was developed with either 3,3′-Diaminobenzidine

(DAB) substrate alone or in some cases DAB substrate plus cobalt and nickel chloride (Roche).

ELISA

The concentration of cytokine in BALF and lung homogenates were determined using OptiEIA Mouse IL-6 ELISA Set (BD Biosciences, San Jose, CA, USA) and Mouse IL-12p40, Mouse IFN-g ELISA kit (eBioscience), and DuoSet Mouse MIP-2 and Mouse KC (R&D Systems Inc., Minneapolis, MN, USA). These assays were performed according to the manufacturers' instructions.

Western Blotting

Western blotting was performed as described previously (10, 48, 49). Briefly, lungs from Cpn infected mice were homogenized and lysed in PLC lysis buffer containing proteinase inhibitors (Protease Inhibitor Cocktail, Sigma-Aldrich). Lung cell lysates and BALF were boiled in sample buffer, and then proteins were separated with SDS-PAGE. Separated proteins were transferred to BioTrace™ PVDF membrane (Pall Corporation, Pensacola, FL). Membranes were probed with anti-mouse Claudin5 Ab (mouse polyclonal) (LifeSpan Biosciences, Seattle, WA, USA), anti-human Claudin18 Ab (rabbit polyclonal) (LifeSpan Biosciences), and anti-mouse MMP9 Ab (rabbit polyclonal) (Abcam, Cambridge, MA, USA) followed by HRP-conjugated goat anti-mouse or anti-rabbit Ab (Thermo Fisher Scientific, Rockford, IL, USA). Chemiluminescence was developed using enhanced Immun-Star™ WesternC™ Kit (BIO-RAD) and documented using ChemiDoc™ XRS+ (Bio-Rad). Densitometry was performed using Image Lab software (ver 3.0, BioRad) and was normalized to b-actin.

Statistics

Data are presented as mean values ±SD. For survival studies, significance was evaluated by Fisher's exact test. Statistical significance was evaluated using Mann-Whitney. For experiments where more than two samples were analyzed, one-way ANOVA with Tukey's post-hoc test was used to assess for statistical significance between groups.

Results

Mast cell-deficient mice are protected from *Chlamydia pneumoniae* lung infection-induced mortality

While mast cells have been reported to be activated during Cpn infection, these data were obtained several weeks after inoculation (18). We therefore infected WT mice (2×10^6 IFU) with Cpn and sacrificed them 4 days after infection. Using flow cytometry we identified mast cells in the lung and did not find a significant change in their numbers at this time (Supplemental Figure 1A). However, using LAMP1 as a marker for degranulation (50, 51), we found that mast cells did appear to be activated during Cpn infection as LAMP1 surface staining increased in these mast cells (Figure 1A). In order to investigate the role mast cells might play during a Cpn infection in mice, we used $Kit^{w\text{-}sh/w\text{-}sh}$ (Wsh) mice, which are deficient for mast cells. WT and Wsh mice were infected with Cpn (5×10^6 IFU/mouse) intratracheally and monitored for mortality. All of the WT mice died of severe Cpn lung

infection by 14 days post infection, while ~50% of the Wsh mice survived until the end of the experiment at day 31 (Figure 1B), suggesting that the lack of mast cells provide a protection from Cpn infection. In order to understand this unexpected observation, we assessed the bacterial burden in the lung from Cpn-infected WT and Wsh at days 3, 5, and 14 post Cpn infection (Figure 1C). We utilized a lower dose of infection for the rest of these studies compared to the mortality experiment (2×10^6 vs. 5×10^6 IFU). There was no significant difference in bacterial number between WT and Wsh at day 3, but at days 5 and 14 there was a significant decrease in Cpn IFU in Wsh mice when compared to WT. We next investigated proinflammatory cytokines (IL-6, IL-12p40, and IFN-γ) that are known to be responsible for Cpn clearance. Wsh mice had increased IL-6 in the lung and increased IL-12p40 in BALF respectively early in infection at day 3 (Figure 1D). Similarly, IL-6 and IL-12p40 were also increased in the lungs at day 5 in Wsh mice compared with WT mice. However, this was reversed by day 14, and Wsh mice had significantly less IL-6 and IL-12p40 in both BALF and lung as compared with WT. Interestingly, there was no difference in the amounts of IFN-γ between Wsh and WT mice 3 and 5 days after infection. IFN-γ is a key mediator of Cpn clearance and the prevention of persistent infection (12, 22–29). However, similar to IL-6 and IL-12p40, IFN-γ concentrations were significantly diminished in BALF at 14 days after infection in Wsh mice. While the reduction in cytokines at day 14 in Wsh mice was likely due to the decreased bacterial burden, we did not find this correlation at 5 days after infection where Wsh mice had increased cytokines, yet a significant decrease in Cpn IFU (Figure 1C and D).

Mast cells enhance immune cell infiltration into the airway

We hypothesized that the number of macrophages and neutrophils would be increased in Wsh compared to WT because we observed that Cpn clearance was faster, and IL-6 and IL-12p40 concentrations were elevated in Wsh compared with WT at early time point in infection. However, there was no difference between Wsh and WT on day 3, but there was a significant reduction in the BALF total cell number in Wsh compared with WT at both 5 and 14 days after infection (Figure 2A). We next determined the inflammatory cell composition in BALF between Wsh and WT mice. We found that on days 5 and 14, the reduction in cell numbers in the BALF could be largely accounted for by the significant decrease in neutrophil numbers along with a reduction in macrophages on day 14 (Figure 2B and Supplemental Figure 2A). Next, we analyzed the immune cell infiltration in the lung tissue. Surprisingly, in contrast to BALF data, total cell number in the lung was significantly increased in Wsh compared with WT at day 3 and showed a similar trend at day 5 (Figure 2C). Macrophage and neutrophil numbers were significantly increased in the lungs 3 and 5 days after infection in Wsh compared with WT mice (Figure 2D and Supplemental Figure 2B–D). There were no significant differences in the numbers of lymphocytes between Wsh and WT mice (Figure 2D), including the number of Tregs (Supplemental Figure 2E). In order to corroborate the differences we found between BALF cells and lung tissue cells in Wsh mice, we measured the concentration of neutrophilic chemokines, KC and MIP-2, in BALF and the lung of WT and Wsh mice (Figure 2E). While the number of neutrophils in BALF from Wsh was reduced, there was significantly more KC in both the BALF and lung homogenates at 3 and 5 days after infection, and the BALF 14 days after infection (Figure 2E). There were no differences between Wsh and WT mice in MIP-2 concentrations on days

3 and 5 after infection. To access whether vascular permeability was affected, we injected Evans blue dye into Cpn-infected mice. Importantly, the vascular permeability was not altered in Wsh mice during Cpn infection (Supplemental Figure 3A and B). While there was no difference in the amount of Evans blue dye in the lungs of WT and Wsh mice, we also measured the amount of dye present in the BALF. Similar to the cellular infiltration data, there was less Evans blue dye in the BALF from Wsh mice compared to WT controls (Supplemental Figure 3C). Collectively, infiltrating immune cells into the airway were decreased in Wsh compared with WT mice, while immune cells in the lung were increased. While pulmonary vascular permeability appeared to be normal, airway permeability was not. At the same time, whereas KC concentrations were increased in both BALF and lung homogenates in Wsh mice, this did not result in increased neutrophils in BALF.

Chlamydial burden is significantly reduced in macrophages and neutrophils in mast cell-deficient mice

Cpn is an obligate intracellular bacteria and needs host cells to replicate itself. Cpn replicates mainly in macrophage/monocytes, neutrophils, and to a lesser degree, epithelial cells (10, 49, 52, 53). We analyzed for the presence of intracellular Cpn by flow cytometry to determine which cells were infected by Cpn in mast cell deficient mice. On Day 3, we did not find any significant differences in Cpn staining in BALF or lung cells between WT and mast cell deficient mice (data not shown). This was not unexpected as both mice had similar bacterial burdens at that time (Figure 1B). Intracellular Cpn staining was mainly restricted to macrophages and not in neutrophils (BALF and lungs). However, while intracellular macrophage Cpn staining was identical at Day 3, macrophages in the lungs of WT mice had an increased Cpn burden (Figure 3A) compared with Wsh mice. By Day 5, there was a significant decrease in the amount of intracellular Cpn staining in Wsh macrophages and neutrophils in both BALF and the lung cells compared with WT (Figure 3B). These data suggest that Cpn infected and replicated in macrophages during the first three days, and then infected newly infiltrating macrophages and neutrophils. However, perhaps with the reduction in macrophages and neutrophils infiltrating into the airways of Wsh mice, Cpn replication was limited due to a lack of sufficient numbers of host immune cells.

Mast cell degranulation is required for Cpn-induced immune cell infiltration into the airspace

Since mast cells seemed to be required for proper immune cell infiltration into the airways of Cpn infected mice, we next investigated the role of mast cell degranulation in this process. In order to address this question, we used Cromolyn, a mast cell degranulation inhibitor (52, 54). WT mice were treated with Cromolyn (3 mg/kg BW) intratracheally a day prior to and one day after Cpn inoculation (Figure 4). Similar to Cpn-infected Wsh, Cromolyn-treated mice displayed reduced total BALF cell number and neutrophil number in BALF (Figure 4A), and relatively increased total cell number in the lung (Figure 4B). KC and MIP-2 were not significantly different between Cromolyn non-treated and treated groups (Figure 4C). Strikingly, Cpn IFU was significantly reduced in Cromolyn-treated mice (Figure 4D).

As our data suggested that mast cell degranulation is required for proper immune infiltration into the airways, we hypothesized that inducing excess degranulation pharmacologically would have the opposite effect with greater numbers of cells in the BALF and an increased bacterial burden. We used Compound 48/80, a mast cell degranulation inducer, to investigate a role of mast cell degranulation against Cpn lung infection (40, 54). WT mice were treated with Compound 48/80 (2 mg/kg BW) intratracheally 2 days after Cpn inoculation followed by sacrifice on day 5. As predicted, Compound 48/80-treated mice displayed increased total cell numbers in the BALF (Figure 5A), whereas the total cell number in the lung was not changed (Figure 5B). Compound 48/80 treated mice also had increased KC in the BALF and MIP-2 in the lung homogenates compared with non-treated mice (Figure 5C). Finally, Cpn IFUs were significantly increased in Compound 48/80-treated mice compared with control mice (Figure 5D). These data suggest that mast cell degranulation plays a role in immune cells infiltration of the airway, and is beneficial for Cpn replication.

Mast cell-deficient mice have impaired immune cell distribution in the lung during Cpn infection

Next, we observed histology of lung tissue from Cpn-infected WT and Wsh. At day 3 post-infection mice had no obvious differences between WT and Wsh mice (data not shown). However, at both days 5 and 14 we found that infiltrating cells had accumulated in a perivascular distribution in Wsh lungs while WT mice showed very little of this phenotype (Figure 6A). Also at days 5 and 14, Wsh lungs displayed patchy inflammatory lesions in lung parenchyma, while WT lung inflammation was much diffuse (Figure 6A). The perivascular accumulations in Wsh mice contained large numbers of B and T cells (Figure 6A). While these structures superficially looked like inducible bronchus associated lymphoid tissues (iBALTs), their appearance by only 5 days after infection precludes them from being a normal iBALT as they are generally a product of a long-term immune response. Additionally, these accumulations did not provide any advantage of acquired immunity later such as Cpn-specific IgG production or effector memory T cells numbers in draining lymph node and IFN-γ production in spleen (data not shown).

Neutrophils staining in the lungs also displayed a patchy distribution in Wsh lungs compared with WT lungs that showed a very diffuse staining pattern (Figure 6B), although the neutrophils were not quite as clustered as the T and B cells were. These data suggest that mast cells play a role for regulating inflammatory cell distribution in the lung and infiltration into the airways.

Mast cell-deficient mice are defective in claudin degradation during Cpn lung infection

Next, we investigated the role of claudins that might play in the defective immune cell infiltration into the airways of Wsh mice. Claudins are important components of tight junctions and their degradation is required for paracellular permeability of not only fluid, but also of immune cells (40). We analyzed claudin 5 and 18 protein levels in the lungs of WT and Wsh mice by Western Blotting. When infected with Cpn, the lungs of Wsh mice displayed significantly reduced claudin degradation (both 5 and 18) in comparison to WT (Figure 7A), although there was no difference in claudin proteins amounts between Wsh and

WT lungs in uninfected animals (Figure 7A). As claudins are degraded by MMP-9 *in vivo* (40, 55, 56), we assayed the presence of MMP-9 in the BALF of infected WT and Wsh mice and found that secreted MMP-9 was indeed reduced in Wsh BALF compared with WT (Figure 7B). Mast cells are known to secrete MMP-9 (32, 55, 56). During degranulation, mast cells also release chymase, a major MMP-9 activator in vivo (30, 32). Thus it is possible that during a Cpn infection in mice, mast cells release and activate MMP-9 (most likely via chymase), which then degrades claudin 5 and 18 in epithelial tight junctions, and allows infiltrating immune cells into the airspaces.

In addition to claudin degradation, triggering receptor expressed on myeloid cells 1 (TREM-1) has been described to be required for neutrophil transepithelial migration in the lung (25, 29, 30). However, we did not find any significant difference in TREM-1 cell-surface expression between WT and Wsh neutrophils in both BALF and lung during infection (data not shown).

Mast cell reconstitution restores WT phenotype to Wsh mice

Wsh mice have an inverted *Kit* gene upstream of the normal gene that leads to selective reduction of Kit expression and resulting MCs deficiency. However, these mice also bear other abnormalities including splenic myeloid and megakaryocytic hyperplasia (57). Therefore, in order to access mast cell deficiency phenotype in Wsh mice, we adoptively transferred WT mast cells into Wsh mice, then infected them with Cpn. Reconstitution with WT mast cells resulted in an increased bacterial burden, similar to WT mice (Figure 8A). Additionally, histopathology revealed similar diffuse immune cell staining to WT mice in MC reconstituted mice (Figure 8B). These data demonstrated that the difference found in bacterial burden in Wsh versus WT mice is solely due to the lack of mast cells, and not any other underlying features in Wsh mice. Mast cell reconstitution also restored claudin 5 degradation and MMP-9 secretion and activation (Figure 8C), highlighting the critical role of mast cells in these processes during Cpn infection.

Discussion

In this study we investigated the role that mast cells play during a Cpn infection of the lung in mice. Using mast cell-deficient mice, we were surprised to discover that Wsh mice were in fact protected from Cpn infection, with decreased mortality, reduced pulmonary inflammation, and lower bacterial titers. These observations were juxtaposed with a decrease in immune cell infiltrates into the airspaces, and an increase in immune cells into the lungs. Interestingly, while there was no difference in vascular permeability between Wsh and WT mice in the whole lung, there was less Evans blue dye detected in the BALF of Wsh mice compared with WT. Histopathology of the lungs revealed Wsh mice to have patchy inflammation with large immune cell clusters in a perivascular distribution while WT mice had a much more diffuse staining pattern. Pharmacological manipulation of mast cells with Cromolyn, a mast cell stabilizer, phenocopied mast cell deficiency with decreased inflammation and bacterial burden, while Compound 48/80, which induces mast cell degranulation, exacerbated infection with increased inflammation and bacterial burden. The results of these pharmacological interventions suggest that mast cell degranulation is

important in the response to Cpn infection, and following bacterial persistence possibly. Mast cell deficiency also coincided with a lack of claudin 5 and 18 degradation in the lungs during Cpn infection, with reduced amounts of MMP-9 in the BALF, suggesting that mast cells maybe required for the opening of tight cell junctions to allow infiltrating immune cells access to the airspaces. Critically, mast cell reconstitution in Wsh mice led to normal bacterial growth, claudin 5 degradation, and increased MMP secretion.

While it's clear that mast cells play a critical role in immune cell recruitment to the airspaces during Cpn infection, it needs further investigation to identify how these mast cells are activated. In our model, it is likely that mast cells are not directly activated by Cpn, but by cytokines produced by immune cells in response to Cpn infection. Peritoneal mast cells exposed to Cpn directly were not activated (data not shown) suggesting a secondary mechanism is at play. Indeed, mast cells have been shown to have far reaching effects, with systemic mast cell activation playing a critical role in local inflammatory responses (58). However, a previous publication did find that human mast cells could produce cytokines in response to CP directly (*in vitro*) and that in a pulmonary Cpn infection in mice, mast cells were observed to be degranulated at a greater rate (18). Thus it may be possible that Cpn infection can induce cytokine production directly, and indirectly induce degranulation. Indeed, we did find evidence for mast cell degranulation 4 days after Cpn infection based upon increased LAMP1 detection on the surface of mast cells in the lung.

In recent studies, mast cells have emerged as an important cell type in both viral and bacterial infections. *Francisella tularensis* can activate mast cells vial TLR2, which then results in enhanced macrophage killing of *Francisella* by secreting IL-4 (25, 29, 59). TNF-α produced by mast cells plays a critical in neutrophil recruitment to the lungs during a *Klebsiella pneumoniae* infection (28, 59). Mast cell-deficient mice are also more susceptible to *Mycoplasma pneumoniae* infection with greater bacterial burden and mortality (28). Dietrich et al found that mast cells are primed to respond to both gram-positive and gram-negative bacteria by the secretion of proinflammatory cytokines (12–14). However, unlike these studies, we found that mast cell-deficient mice were protected from mortality and had a reduced Cpn burden in the lungs. This is somewhat similar to the role mast cells play during influenza A virus infection in mice. Mast cell-deficient mice were protected from body weight loss and inflammation when infected with H1N1 influenza A virus (14, 15). However, despite the lack of inflammation, there was no difference in viral titers in that model. It might come from the difference of the target cells between Cpn and H1N1 influenza A that infects epithelial cells more than macrophages (60). Thus while there seems to be a general consensus that mast cells induce a potent inflammatory response to infection, depending on the organism, this inflammation can be either beneficial, damaging, or as in our study, lead to unproductive inflammation and greater bacterial growth. Indeed, in a recent study, mast cell-deficient mice were protected from *Streptococcus pneumoniae* pneumonia, although this was independent of mast cell degranulation (61). *Chlamydia pneumoniae* requires host cells for productive replication. Initial pulmonary infection occurs mainly in alveolar macrophages, and to a lesser degree, epithelial cells. In our study, mast cells facilitated the influx of neutrophils and other macrophage/monocytes into the airspaces where the bacterial progeny of the first round of replication could now infect them, leading

to a longer and more damaging infection. Indeed, it was previously reported that neutrophil depletion promotes bacterial clearance during Cpn lung infection (10, 16, 17) and that neutrophils are a critical site of Cpn replication (62, 63), again suggesting that neutrophils play an important role as an infectious target of Cpn.

The key to the protection found against Cpn infection in mast cell-deficient mice was primarily the lack of immune cell recruitment to the airspaces, despite increased chemokine production. In other models, mast cells were found to be important in immune cell recruitment. In the EAE model of multiple sclerosis, mast cells in the dura mater and pia mater exacerbate the inflammation by facilitating neutrophil recruitment and promoting blood brain barrier and CSF-blood barrier breakdown to allow immune cells access to the CNS (19–21). Additionally, in a *Pseudomonas* LPS model of pulmonary inflammation, mast cells mediated the influx of neutrophils into the lung (12, 24–29). One possible mechanism for the control of neutrophil infiltration into the lungs was by controlling TREM-1 expression on neutrophils. TREM-1 was found to be required for transepithelial migration of neutrophils (30). However, we did not find any differences in TREM-1 expression in neutrophils in mast cell deficient mice, indicating that the regulation of immune cell infiltration by mast cells in Cpn infection is independent of TREM-1. Additionally, mast cell deficient mice also displayed abnormal T and B cell distribution in the lung later in the course of Cpn infection, suggesting that the mast cells regulate not only neutrophil transmigration, but also other cell migration during infection.

Mast cells can make and secrete chymase, a critical protease that can activate many other cellular products by their cleavage (32). One such downstream product is MMP-9, an important metallo-proteinase that is responsible for cleaving many surface exposed cellular proteins (35). In our study, we found that MMP-9 was present in the BALF of WT infected mice, and was drastically reduced in mast cell-deficient mice. One function of MMP-9 is to breakdown tight junctions, thus allowing cellular infiltration (35). Claudins are a group of extracellular adhesions proteins responsible for tight junction formation (38) and MMP-9 has been shown degrade claudins in epithelial tight junctions to allow transepithelial migration of immune cells (39, 40). Our data clearly showed that during a Cpn infection in mice, both claudin 5 and 18 were degraded in the lungs, and that Wsh mice were protected from this degradation. Reconstitution of mast cells led to the restoration of claudin 5 degradation and MMP9 secretion concomitantly with an increased bacterial burden, similar to WT. We therefore propose that the lack of immune cell infiltrates into the airways in mast cell deficient mice during Cpn infection is due to the inability of the host to breakdown the epithelial cell tight junctions as a consequence of the lack of mast cell-derived MMP-9. While a disrupted chemokine gradient could also explain the reduction in immune cell infiltrates into the airspaces, there was actually increased KC in BALF and lungs suggesting that this is not the case. While migration of cells into the airspaces was inhibited in mast cell-deficient mice, the clusters of B and T cells were more pronounced than that of the neutrophils as seen by histology. It is possible that the neutrophils achieved a slightly more diffuse staining pattern compared with that of B and T cells as they can secrete their own MMP-9 (37, 64, 65), which may allow them to migrate slightly more interstitially than the B and T cells. It is also possible that it is the neutrophilic MMP-9 that is necessary for claudin

degradation. However, as there are actually more neutrophils in the lungs of the infected Wsh mice, this seems less likely. Alternatively, it could be that the neutrophils are not activated, but this would still place them downstream of mast cells in the immune response.

One caveat to our experiments was the use of the Kit$^{W\text{-}sh/W\text{-}sh}$ mouse model. Several recent studies have found that in some cases, mast cell deficiency was not the reason for the observed phenotype, but it was the mutation itself affecting other developmental pathways (43). Of potential concern was the finding that these mice may have differential Treg numbers and activity. In one study investigating oral tolerance, both Kit$^{W\text{-}sh/W\text{-}sh}$ and Kit$^{W/W\text{-}v}$ mice had increased numbers of Tregs that was not affected by mast cell reconstitution (44). Another study found an opposite result, with greatly reduced Treg numbers leading to greater inflammation in Kit$^{W\text{-}sh/W\text{-}sh}$ mice (45). However, in our experiments we did not find any difference in Tregs in the lungs of our infected WT and mast cell deficient mice (Supplementary Figure 2E). It was also reported that Kit$^{W\text{-}sh/W\text{-}sh}$ mice frequently develop myeloid and megakaryocytic proliferation in the spleen and bone marrow, resulting in neutrophilia, basophilia, increased mast cell progenitor numbers in the spleen and elevated platelet numbers in the blood (47). Nevertheless, our study demonstrated that Kit$^{W\text{-}sh/W\text{-}sh}$ mice had less neutrophil migration in alveoli. Furthermore, pharmacological intervention of WT mice during Cpn infection both phenocopied mast cell deficiency (cromolyn), or led to greater inflammation and greater bacterial burden (compound 48/80) (Figure 4 and 5). Finally, MCs reconstitution restored phenotypic features of Cpn infection indicating that it is unlikely that our observations regarding using Kit$^{W\text{-}sh/W\text{-}sh}$ are due to any other potential inherent defect in these mice, and are due to the lack of mast cells and their responses during Cpn infection. Finally, while certain mast cell deficient mice (i.e. WBB6F1-Kit$^{W/W\text{-}v}$) were reported to have associated neutropenia, the mice we used (C57BL/6-Kit$^{W\text{-}sh/W\text{-}sh}$) do not and instead have increased numbers of neutrophils, which we did find in the lungs (66). Thus, while we do not believe intrinsic PMNs alterations affected our observations on the role of mast cells, we cannot completely rule out this possibility.

Chlamydia pneumoniae remains an enigmatic infectious organism with associations to many important human diseases. Understanding this unique organisms complex lifecycle and the immune systems response to infection is a high priority. In this study we found that the normal immune response is actually beneficial to Cpn infection by providing Cpn with host cells to infect and propagate. Without the presence of mast cells, inflammation was mild, mortality was reduced, and Cpn was rapidly cleared from the hosts. Not only do these studies provide important new paradigms for how we understand infections, they may provide new avenues of treatments and protective strategies. Additionally, while mast cells have long been considered to primarily play a role in Th2-mediated diseases, they have been revealed to be major players in both inflammatory disorders and infections. Our findings place mast cells as critical gatekeepers during a pulmonary bacterial infection, facilitating immune cell transepithelial migration in the lungs into the airways, and thus provides a new target for intervention strategies.

Supplementary Material

Refer to Web version on PubMed Central for supplementary material.

Acknowledgments

This work was supported by National Institutes of Health (NIH) grants AI-067995 and 2R56AI067995-06 to M.A.

We thank Ganghua Huang, Wenxuan Zhang, and Polly Sun for experimental assistance. We also thank Dr. Barry Stripp and William Parks (Cedars-Sinai Medical Center, Department of Pulmonary Medicine) for their critical reading of this manuscript.

References

1. Kuo CC, Jackson LA, Campbell LA, Grayston JT. Chlamydia pneumoniae TWAR. Clin Microbiol Rev. 1995; 8:451–461. [PubMed: 8665464]
2. Teh B, Grayson ML, Johnson RPD, Charles PPG. Doxycycline vs. macrolides in combination therapy for treatment of community-acquired pneumonia. Clin Microbiol Infect. 2012; 18:E71–3. [PubMed: 22284533]
3. Sutherland ER, Martin RJ. Asthma and atypical bacterial infection. Chest. 2007; 132:1962–1966. [PubMed: 18079229]
4. Watson C, Alp NJ. Role of Chlamydia pneumoniae in atherosclerosis. Clin Sci. 2008; 114:509–531. [PubMed: 18336368]
5. Naiki Y, Sorrentino R, Wong MH, Michelsen KS, Shimada K, Chen S, Yilmaz A, Slepenkin A, Schröder JNW, Crother TR, Bulut Y, Doherty TM, Bradley M, Shaposhnik Z, Peterson EM, Tontonoz P, Shah PK, Arditi M. TLR/MyD88 and liver X receptor alpha signaling pathways reciprocally control Chlamydia pneumoniae-induced acceleration of atherosclerosis. The Journal of Immunology. 2008; 181:7176–7185. [PubMed: 18981139]
6. Schröder NWJ, Crother TR, Naiki Y, Chen S, Wong MH, Yilmaz A, Slepenkin A, Schulte D, Alsabeh R, Doherty TM, Peterson EM, Nel AE, Arditi M. Innate immune responses during respiratory tract infection with a bacterial pathogen induce allergic airway sensitization. J Allergy Clin Immunol. 2008; 122:595–602.e5. [PubMed: 18774395]
7. Grayston JT. Background and current knowledge of Chlamydia pneumoniae and atherosclerosis. J INFECT DIS. 2000; 181(Suppl 3):S402–10. [PubMed: 10839724]
8. Naiki Y, Michelsen KS, Schröder JNW, Alsabeh R, Slepenkin A, Zhang W, Chen S, Wei B, Bulut Y, Wong MH, Peterson EM, Arditi M. MyD88 is pivotal for the early inflammatory response and subsequent bacterial clearance and survival in a mouse model of Chlamydia pneumoniae pneumonia. J Biol Chem. 2005; 280:29242–29249. [PubMed: 15964841]
9. Rodriguez N, Wantia N, Fend F, Dürr S, Wagner H, Miethke T. Differential involvement of TLR2 and TLR4 in host survival during pulmonary infection with Chlamydia pneumoniae. Eur J Immunol. 2006; 36:1145–1155. [PubMed: 16609927]
10. Shimada K, Chen S, Dempsey PW, Sorrentino R, Alsabeh R, Slepenkin AV, Peterson EM, Doherty TM, Underhill D, Crother TR, Arditi M. The NOD/RIP2 pathway is essential for host defenses against Chlamydophila pneumoniae lung infection. PLoS Pathog. 2009; 5:e1000379. [PubMed: 19360122]
11. Shimada K, Crother TR, Arditi M. Innate immune responses to Chlamydia pneumoniae infection: role of TLRs, NLRs, and the inflammasome. Microbes Infect. 2012; 14:1301–1307. [PubMed: 22985781]
12. Dietrich N, Rohde M, Geffers R, Kröger A, Hauser H, Weiss S, Gekara NO. Mast cells elicit proinflammatory but not type I interferon responses upon activation of TLRs by bacteria. Proc Natl Acad Sci USA. 2010
13. He X, Mekasha S, Mavrogiorgos N, Fitzgerald KA, Lien E, Ingalls RR. Inflammation and fibrosis during Chlamydia pneumoniae infection is regulated by IL-1 and the NLRP3/ASC inflammasome. The Journal of Immunology. 2010; 184:5743–5754. [PubMed: 20393140]

14. Shimada K, Crother TR, Karlin J, Chen S, Chiba N, Ramanujan VK, Vergnes L, Ojcius DM, Arditi M. Caspase-1 dependent IL-1β secretion is critical for host defense in a mouse model of Chlamydia pneumoniae lung infection. PLoS ONE. 2011; 6:e21477. [PubMed: 21731762]
15. Graham AC, Hilmer KM, Zickovich JM, Obar JJ. Inflammatory Response of Mast Cells during Influenza A Virus Infection Is Mediated by Active Infection and RIG-I Signaling. The Journal of Immunology. 2013
16. Rodriguez N, Fend F, Jennen L, Schiemann M, Wantia N, Prazeres da Costa CU, Dürr S, Heinzmann U, Wagner H, Miethke T. Polymorphonuclear neutrophils improve replication of Chlamydia pneumoniae in vivo upon MyD88-dependent attraction. J Immunol. 2005; 174:4836–4844. [PubMed: 15814710]
17. Crother TR, Ma J, Jupelli M, Chiba N, Chen S, Slepenkin A, Alsabeh R, Peterson E, Shimada K, Arditi M. Plasmacytoid dendritic cells play a role for effective innate immune responses during Chlamydia pneumoniae infection in mice. PLoS ONE. 2012; 7:e48655. [PubMed: 23119083]
18. Oksaharju A, Lappalainen J, Tuomainen AM, Pussinen PJ, Puolakkainen M, Kovanen PT, Lindstedt KA. Pro-atherogenic lung and oral pathogens induce an inflammatory response in human and mouse mast cells. J Cell Mol Med. 2009; 13:103–113. [PubMed: 18298659]
19. Christy AL, Walker ME, Hessner MJ, Brown MA. Mast cell activation and neutrophil recruitment promotes early and robust inflammation in the meninges in EAE. J Autoimmun. 2012
20. Nakamura Y, Kambe N, Saito M, Nishikomiri R, Kim Y, Murakami M, Núñez G, Matsue H. Mast cells mediate neutrophil recruitment and vascular leakage through the NLRP3 inflammasome in histamine-independent urticaria. J Exp Med. 2009
21. Matsuguchi T. Mast cells as critical effectors of host immune defense against Gram-negative bacteria. Curr Med Chem. 2012; 19:1432–1442. [PubMed: 22360480]
22. Urb M, Sheppard C Donald. The Role of Mast Cells in the Defence against Pathogens. PLoS Pathog. 2012:1–3.
23. Rottenberg ME, Gigliotti-Rothfuchs A, Wigzell H. The role of IFN-gamma in the outcome of chlamydial infection. Current Opinion in Immunology. 2002; 14:444–451. [PubMed: 12088678]
24. Lê BV, Khorsi-Cauet H, Bach V, Gay-Quéheillard J. Mast cells mediate Pseudomonas aeruginosa lipopolysaccharide-induced lung inflammation in rat. Eur J Clin Microbiol Infect Dis. 2012; 31:1983–1990. [PubMed: 22282020]
25. Rodriguez AR, Yu J-J, Guentzel MN, Navara CS, Klose KE, Forsthuber TG, Chambers JP, Berton MT, Arulanandam BP. Mast Cell TLR2 Signaling Is Crucial for Effective Killing of Francisella tularensis. The Journal of Immunology. 2012
26. Dudeck A, Suender CA, Kostka SL, von Stebut E, Maurer M. Mast cells promote Th1 and Th17 responses by modulating dendritic cell maturation and function. Eur J Immunol. 2011
27. Echtenacher B, Männel DN, Hültner L. Critical protective role of mast cells in a model of acute septic peritonitis. Nature. 1996; 381:75–77. [PubMed: 8609992]
28. Xu X, Zhang D, Lyubynska N, Wolters PJ, Killeen NP, Baluk P, McDonald DM, Hawgood S, Caughey GH. Mast cells protect mice from Mycoplasma pneumonia. Am J Respir Crit Care Med. 2006; 173:219–225. [PubMed: 16210667]
29. Ketavarapu JM, Rodriguez AR, Yu J-J, Cong Y, Murthy AK, Forsthuber TG, Guentzel MN, Klose KE, Berton MT, Arulanandam BP. Mast cells inhibit intramacrophage Francisella tularensis replication via contact and secreted products including IL-4. Proceedings of the National Academy of Sciences. 2008; 105:9313–9318.
30. Klesney-Tait J, Keck K, Li X, Gilfillan S, Otero K, Baruah S, Meyerholz DK, Varga SM, Knudson CJ, Moninger TO, Moreland J, Zabner J, Colonna M. Transepithelial migration of neutrophils into the lung requires TREM-1. J Clin Invest. 2013; 123:138–149. [PubMed: 23241959]
31. Vartio T, Seppä H, Vaheri A. Susceptibility of soluble and matrix fibronectins to degradation by tissue proteinases, mast cell chymase and cathepsin G. J Biol Chem. 1981; 256:471–477. [PubMed: 6450204]
32. Caughey GH. Mast cell tryptases and chymases in inflammation and host defense. Immunol Rev. 2007; 217:141–154. [PubMed: 17498057]

33. Fang KC, Raymond WW, Lazarus SC, Caughey GH. Dog mastocytoma cells secrete a 92-kD gelatinase activated extracellularly by mast cell chymase. J Clin Invest. 1996; 97:1589–1596. [PubMed: 8601622]
34. Tchougounova E, Lundequist A, Fajardo I, Winberg J-O, Åbrink M, Pejler G. A key role for mast cell chymase in the activation of pro-matrix metalloprotease-9 and pro-matrix metalloprotease-2. J Biol Chem. 2005; 280:9291–9296. [PubMed: 15615702]
35. Parks WC, Shapiro SD. Matrix metalloproteinases in lung biology. Respir Res. 2001; 2:10–19. [PubMed: 11686860]
36. Oyamada S, Bianchi C, Takai S, Chu LM, Sellke FW. Chymase inhibition reduces infarction and matrix metalloproteinase-9 activation and attenuates inflammation and fibrosis after acute myocardial ischemia/reperfusion. J Pharmacol Exp Ther. 2011; 339:143–151. [PubMed: 21795433]
37. Bradley LM, Douglass MF, Chatterjee D, Akira S, Baaten GBJ. Matrix metalloprotease 9 mediates neutrophil migration into the airways in response to influenza virus-induced toll-like receptor signaling. PLoS Pathog. 2012; 8:e1002641. [PubMed: 22496659]
38. Wang F, Daugherty B, Keise LL, Wei Z, Foley JP, Savani RC, Koval M. Heterogeneity of claudin expression by alveolar epithelial cells. Am J Respir Cell Mol Biol. 2003; 29:62–70. [PubMed: 12600828]
39. Ichiyasu H, McCormack JM, McCarthy KM, Dombkowski D, Preffer FI, Schneeberger EE. Matrix metalloproteinase-9-deficient dendritic cells have impaired migration through tracheal epithelial tight junctions. Am J Respir Cell Mol Biol. 2004; 30:761–770. [PubMed: 14656746]
40. Chiu P-S, Lai S-C. Matrix metalloproteinase-9 leads to claudin-5 degradation via the NF-κB pathway in BALB/c mice with eosinophilic meningoencephalitis caused by Angiostrongylus cantonensis. PLoS ONE. 2013; 8:e53370. [PubMed: 23505411]
41. Armstrong SM, Wang C, Tigdi J, Si X, Dumpit C, Charles S, Gamage A, Moraes TJ, Lee WL. Influenza infects lung microvascular endothelium leading to microvascular leak: role of apoptosis and claudin-5. PLoS ONE. 2012; 7:e47323. [PubMed: 23115643]
42. Ohta H, Chiba S, Ebina M, Furuse M, Nukiwa T. Altered expression of tight junction molecules in alveolar septa in lung injury and fibrosis. AJP: Lung Cellular and Molecular Physiology. 2012; 302:L193–205. [PubMed: 22003091]
43. Rodewald H-R, Feyerabend TB. Widespread immunological functions of mast cells: fact or fiction? Immunity. 2012; 37:13–24. [PubMed: 22840840]
44. Tunis MC, Dawicki W, Carson KR, Wang J, Marshall JS. Mast cells and IgE activation do not alter the development of oral tolerance in a murine model. J Allergy Clin Immunol. 2012; 130:705–715.e1. [PubMed: 22607990]
45. Piconese S, Costanza M, Musio S, Tripodo C, Poliani PL, Gri G, Burocchi A, Pittoni P, Gorzanelli A, Colombo MP, Pedotti R. Exacerbated experimental autoimmune encephalomyelitis in mast-cell-deficient Kit W-sh/W-sh mice. Laboratory Investigation. 2011; 91:627–641. [PubMed: 21321538]
46. Peterson EM, Zhong GM, Carlson E, de la Maza LM. Protective role of magnesium in the neutralization by antibodies of Chlamydia trachomatis infectivity. Infect Immun. 1988; 56:885–891. [PubMed: 3346076]
47. Mancardi DA, Jönsson F, Iannascoli B, Khun H, van Rooijen N, Huerre M, Daëron M, Bruhns P. Cutting Edge: The murine high-affinity IgG receptor FcγRIV is sufficient for autoantibody-induced arthritis. The Journal of Immunology. 2011; 186:1899–1903. [PubMed: 21248252]
48. Chiba N, Masuda A, Yoshikai Y, Matsuguchi T. Ceramide inhibits LPS-induced production of IL-5, IL-10, and IL-13 from mast cells. J Cell Physiol. 2007; 213:126–136. [PubMed: 17458900]
49. Blasi F, Centanni S, Allegra L. Chlamydia pneumoniae: crossing the barriers? Eur Respir J. 2004; 23:499–500. [PubMed: 15083742]
50. Cheng LE, Hartmann K, Roers A, Krummel MF, Locksley RM. Perivascular mast cells dynamically probe cutaneous blood vessels to capture immunoglobulin E. Immunity. 2013; 38:166–175. [PubMed: 23290520]

51. Föger N, Jenckel A, Orinska Z, Lee K-H, Chan AC, Bulfone-Paus S. Differential regulation of mast cell degranulation versus cytokine secretion by the actin regulatory proteins Coronin1a and Coronin1b. Journal of Experimental Medicine. 2011; 208:1777–1787. [PubMed: 21844203]
52. Zsámboki G. The pharmacology of sodium cromoglycate. Ther Hung. 1994; 42:37–40. [PubMed: 7761962]
53. Gieffers J, van Zandbergen G, Rupp J, Sayk F, Kruger S, Ehlers S, Solbach W, Maass M. Phagocytes transmit Chlamydia pneumoniae from the lungs to the vasculature. Eur Respir J. 2004; 23:506–510. [PubMed: 15083745]
54. Koibuchi Y, Ichikawa A, Nakagawa M, Tomita K. Histamine release induced from mast cells by active components of compound 48/80. Eur J Pharmacol. 1985; 115:163–170. [PubMed: 2415369]
55. Kanbe N, Tanaka A, Kanbe M, Itakura A, Kurosawa M, Matsuda H. Human mast cells produce matrix metalloproteinase 9. Eur J Immunol. 1999; 29:2645–2649. [PubMed: 10458779]
56. Tanaka A, Arai K, Kitamura Y, Matsuda H. Matrix metalloproteinase-9 production, a newly identified function of mast cell progenitors, is downregulated by c-kit receptor activation. Blood. 1999; 94:2390–2395. [PubMed: 10498611]
57. Katz HR, Austen KF. Mast cell deficiency, a game of kit and mouse. Immunity. 2011; 35:668–670. [PubMed: 22118523]
58. Seeley EJ, Sutherland RE, Kim SS, Wolters PJ. Systemic mast cell degranulation increases mortality during polymicrobial septic peritonitis in mice. Journal of Leukocyte Biology. 2011; 90:591–597. [PubMed: 21653231]
59. Malaviya R, Ikeda T, Ross E, Abraham SN. Mast cell modulation of neutrophil influx and bacterial clearance at sites of infection through TNF-alpha. Nature. 1996; 381:77–80. [PubMed: 8609993]
60. Tate MD, Brooks AG, Reading PC. Inhibition of lectin-mediated innate host defences in vivo modulates disease severity during influenza virus infection. Immunol Cell Biol. 2011; 89:482–491. [PubMed: 20938455]
61. van den Boogaard FE, Brands X, Roelofs JJTH, de Beer R, De Boer OJ, Van't Veer C, van der Poll T. Mast cells impair host defense during murine Streptococcus pneumoniae pneumonia. J INFECT DIS. 2014:jiu285.
62. Rupp J, Pfleiderer L, Jugert C, Moeller S, Klinger M, Dalhoff K, Solbach W, Stenger S, Laskay T, van Zandbergen G. Chlamydia pneumoniae hides inside apoptotic neutrophils to silently infect and propagate in macrophages. PLoS ONE. 2009; 4:e6020. [PubMed: 19547701]
63. van Zandbergen G, Gieffers J, Kothe H, Rupp J, Bollinger A, Aga E, Klinger M, Brade H, Dalhoff K, Maass M, Solbach W, Laskay T. Chlamydia pneumoniae multiply in neutrophil granulocytes and delay their spontaneous apoptosis. J Immunol. 2004; 172:1768–1776. [PubMed: 14734760]
64. Masure S, Proost P, Van Damme J, Opdenakker G. Purification and identification of 91-kDa neutrophil gelatinase. Release by the activating peptide interleukin-8. Eur J Biochem. 1991; 198:391–398. [PubMed: 1645657]
65. Opdenakker G, Van den Steen PE, Van Damme J. Gelatinase B: a tuner and amplifier of immune functions. Trends Immunol. 2001; 22:571–579. [PubMed: 11574282]
66. Reber LL, Marichal T, Galli SJ. New models for analyzing mast cell functions in vivo. Trends Immunol. 2012; 33:613–625. [PubMed: 23127755]

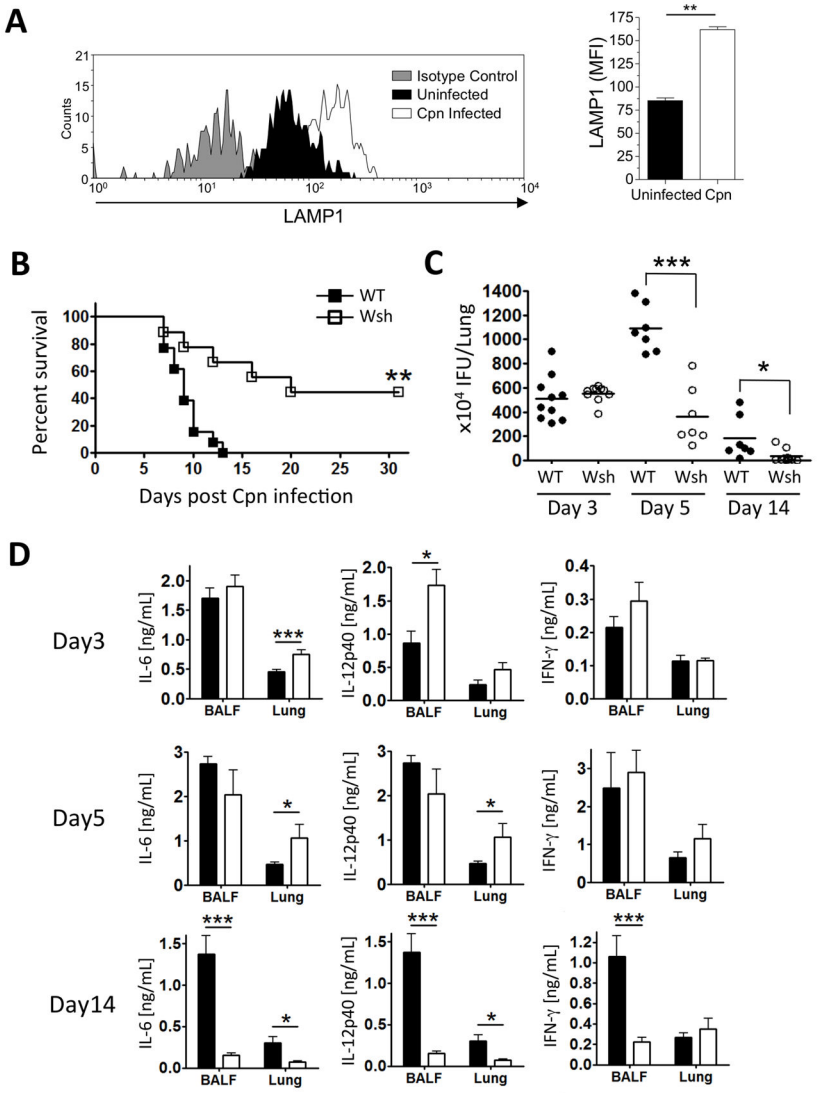

Figure 1. Wsh mice are protected from Cpn-induced mortality and Cpn propagation in the lung compared to WT

(A) WT mice were infected with Cpn (2×10^6 IFU) or mock infected, and sacrificed 4 days later. Single cells from the lung were prepared as described in Material and Methods. Mast cells were identified as side scatter high, c-kit IgE double positive (Supplemental Figure 1A). Surface expression levels of LAMP1 were assessed by flow cytometry and reported as the mean fluorescence intensity (MFI). (B–D) WT and Wsh mice were infected with Cpn intratracheally (5×10^6 IFU for mortality and 2×10^6 for others). (B) Cpn-induced mortality was observed by 31 days post Cpn inoculation. (C) Cpn IFU in the lung from Cpn-infected WT and Wsh was quantified as described in Materials and Methods. (D) BALF was collected from euthanized mice, and the lung was perfused with cold PBS and homogenized. For A, this experiment was performed one time n=5. For B, this experiment was performed twice and the data was pooled together for a total n=13 (WT) and n=10 (Wsh). For C & D the experiment was performed 3 times and the data was pooled for a total n=10 (WT and Wsh) day 3, n=7 (WT and Wsh) day 5, and n=7 (WT) n=10 (Wsh) day 14. Cytokine

concentration in BALF and lung homogenates was detected by ELISA. Data are mean ±SD. Significance of differences was determined by Mann-Whitney. *P<0.05, **P<0.005, ***P<0.001.

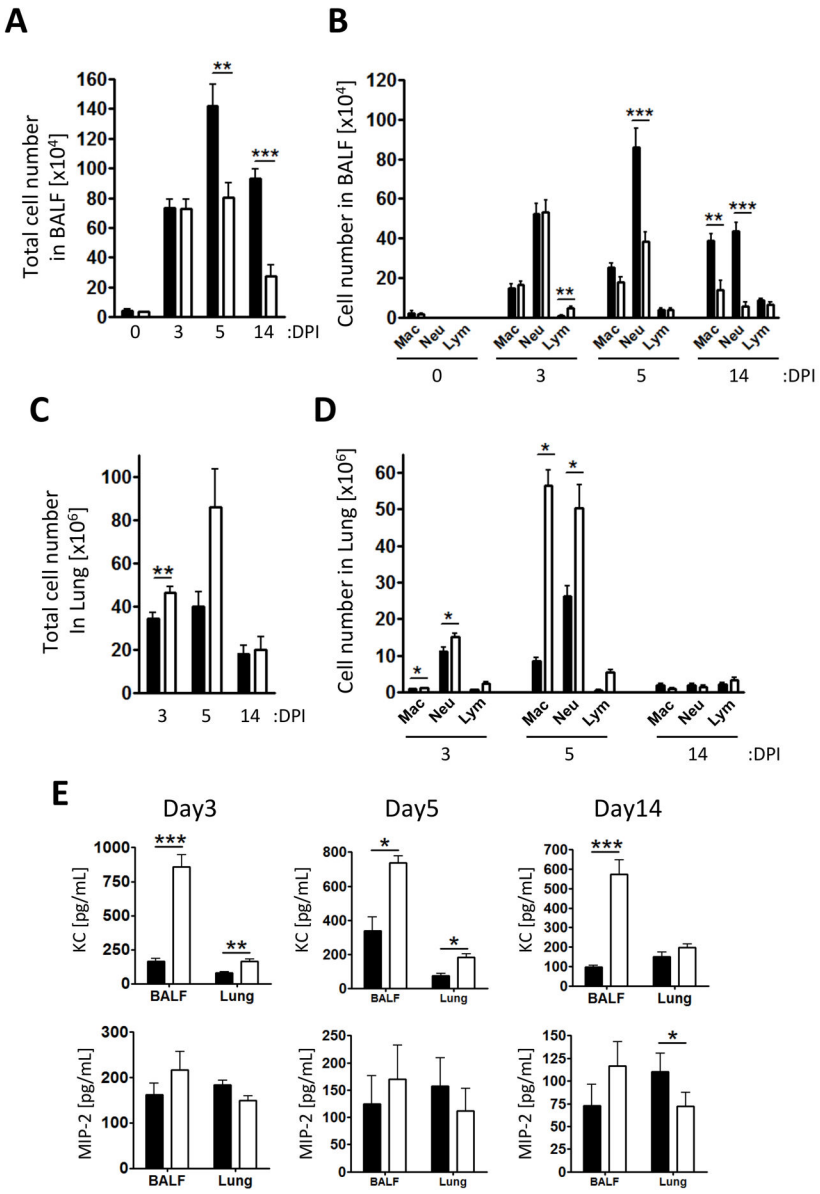

Figure 2. Wsh mice displayed reduced inflammatory cell infiltration into the airspace compared to WT

WT (closed bar) and Wsh (open bar) mice were infected with 2×10^6 Cpn intratracheally. BALF was collected from euthanized mice on 3, 5, and 14 days post Cpn propagation. Total (A) and differential (B) cell counts in BALF. Cell types in BALF were determined by modified Wright-Giemza staining. (C and D) Single cells from lung were collected through enzymatic procedure and analyzed by flow cytometry. (E) Chemokine concentrations in BALF and the lung homogenates were determined by ELISA. This experiment was performed 3 times and the data was pooled for a total n=7 (WT and Wsh) day 0, n=10 (WT) and n=8 (Wsh) day 3, n=9 (WT and Wsh) day 5, and n=7 (WT) n=9 (Wsh) day 14. Data are mean ±SD. Significance of differences was determined by Mann-Whitney. **P*<0.05, ***P*<0.005, ****P*<0.001.

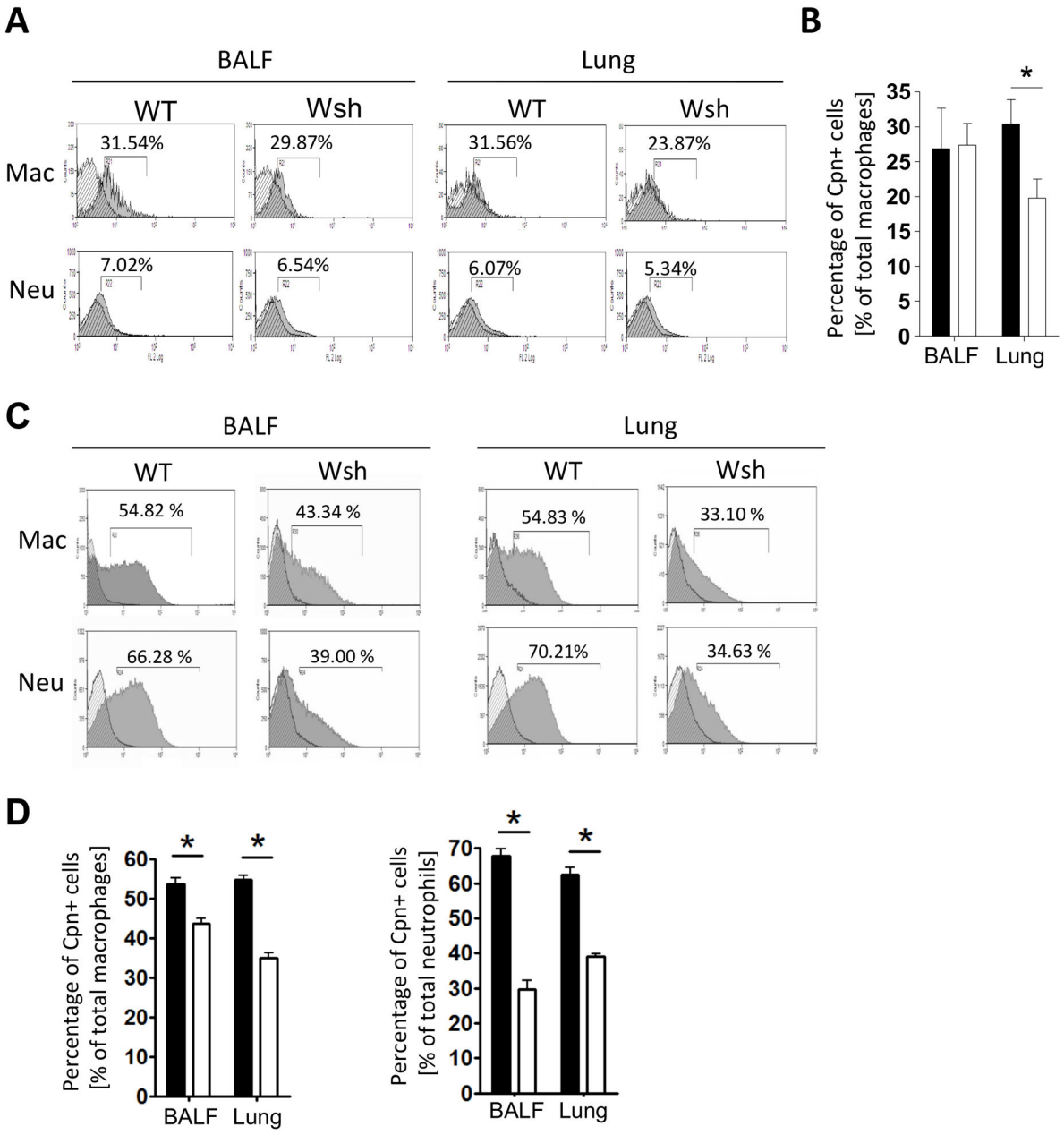

Figure 3. Cpn-positive macrophages and neutrophils were reduced in Wsh compared to WT

WT and Wsh mice were infected with 2×10^6 IFU Cpn intratracheally. Mice were sacrificed either 3 or 5 days post Cpn infection. BAL cells and lung cells were collected at day 3 (A, B) or day 5 (B, D) and stained with anti-Cpn, anti-CD11c, anti CD11b, anti-F4/80, and anti-Ly6G for flow cytometric analysis as before. A) Representative histograms for Cpn staining in gated populations (see Supplementary Figure 1 for gating strategy). B) The percent of Cpn+ cells in the BALF and Lung at day 3. C) Representative histograms for Cpn staining in gated populations on day 5. D) The percent of Cpn+ cells in the BALF and Lung at day 5. For A and B, the experiment was performed twice n=5 (WT) n=6 (wsh). For C and D, the experiment was performed twice n=4 (WT) n=4 (wsh). Data shown is a representative

experiment. Data are mean ±SD. Significance of differences was determined by Mann-Whitney. *P<0.05.

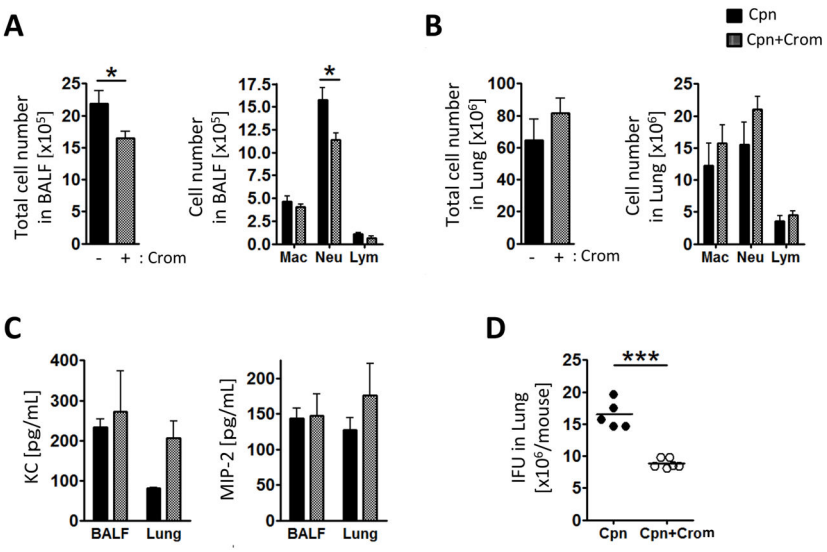

Figure 4. Cromolyn reduces inflammatory cell infiltration into the airspace and bacterial number in the lung

WT mice were treated with cromolyn (3 mg/kg body weight) prior and post Cpn infection (2×10^6 IFU) and sacrificed 5 days post infection. (A) Total and differential cell counts in BALF. Cell types in BALF were determined by modified Wright-Giemza staining. (B) Single cells from lung were collected through enzymatic procedure and analyzed by flow cytometry for differential cell counts. (C) Chemokine concentrations in BALF and the lung homogenates were determined by ELISA. (D) Cpn IFU in the lungs were quantified as described in Materials and Methods. For A–D, this experiment was performed twice n=5 (Cpn) n=6 (Cpn + Cro). Data shown is a representative experiment. Data are mean ±SD. Significance of differences was determined by Mann-Whitney. **P*<0.05, ****P*<0.001.

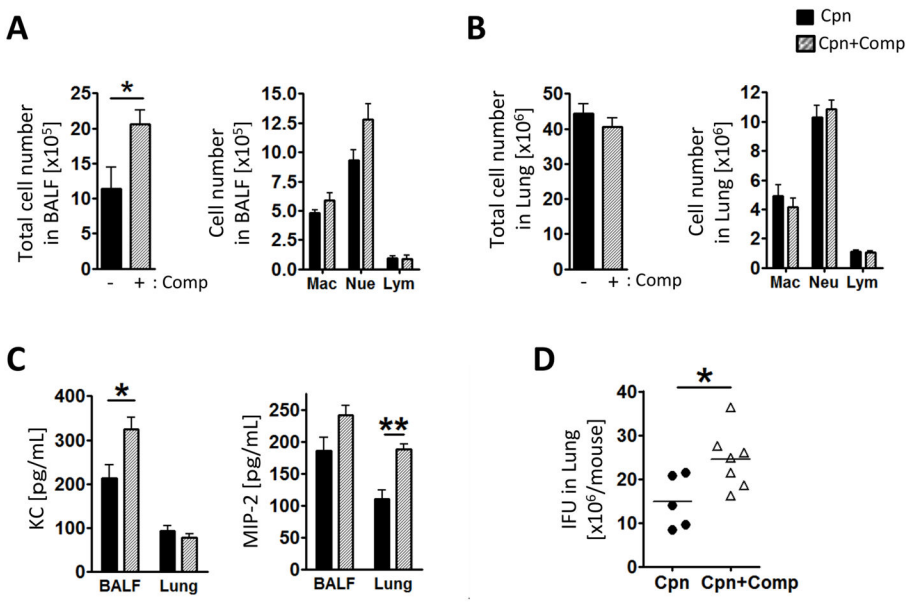

Figure 5. Compound 48/80 increased inflammatory cell infiltration into the airspace and bacterial number in the lung

WT mice were treated with compound 48/80 (2 mg/kg body weight) 2 days post Cpn infection and sacrificed on day 5. Total (A) and differential cell counts in BALF. Cell types in BALF were determined by modified Wright-Giemza staining. (B) Single cells from lung were collected through enzymatic procedure and analyzed by flow cytometry. (C) Chemokine concentrations in BALF and the lung homogenates were determined by ELISA. (D) Cpn IFU in the lung from Cpn-infected WT and Wsh was quantified as described in Materials and Methods. For A–D, this experiment was performed twice n=5 (Cpn) n=7 (Cpn + Compound 48/80). Data shown is a representative experiment. Data are mean ±SD. Significance of differences was determined by Mann-Whitney. **P*<0.05, ****P*<0.001.

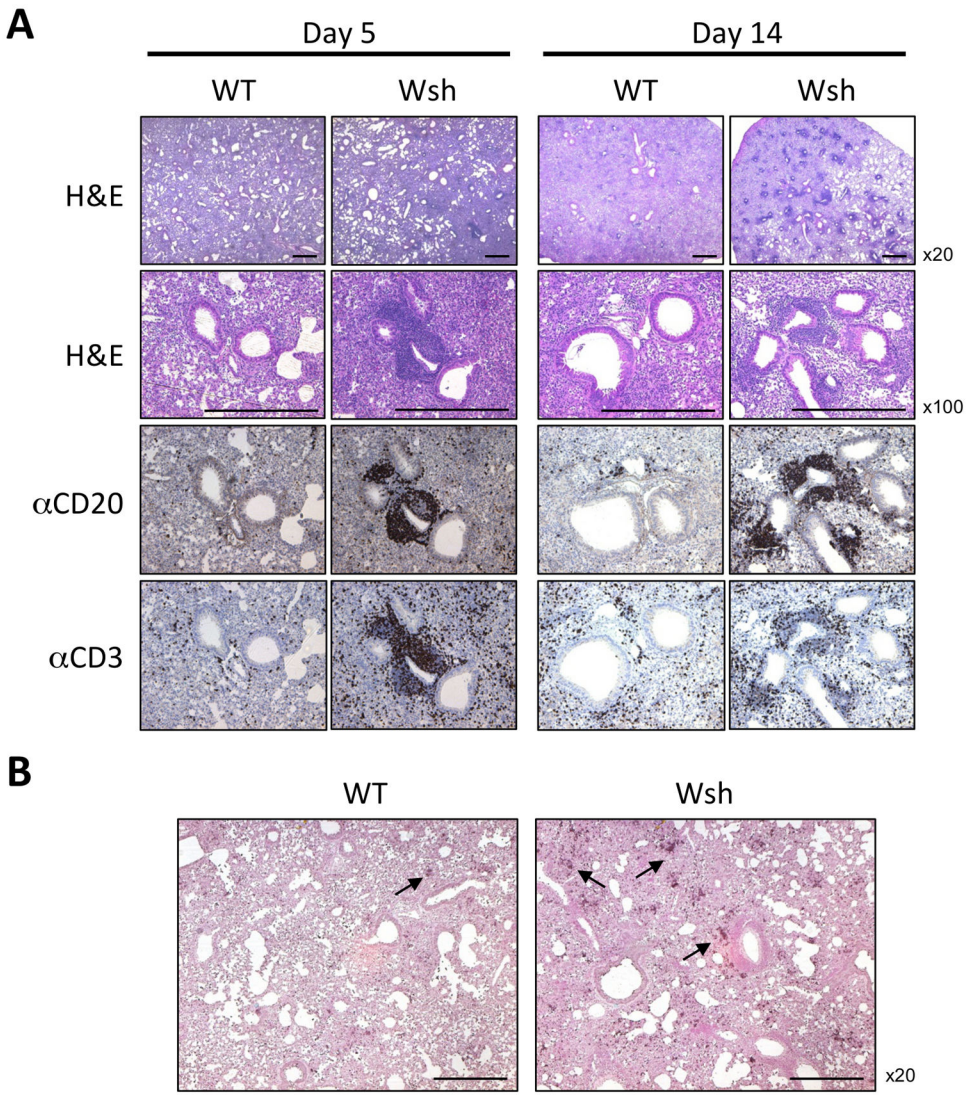

Figure 6. Wsh mice displayed patchy inflammation and accumulated T and B cells perivascularly and accumulated neutrophils in the lung during Cpn-induced lung inflammation

WT and Wsh mice were infected with Cpn intratracheally. Lungs were harvested for HE staining and immunohistochemistry for B cells and T cells on day 5 and day 14 (A) and neutrophils on day 5 (B). This experiment was performed 3 times and the data was pooled for a total n=7 (WT and Wsh) day 5, and n=7 (WT) n=10 (Wsh) day 14. Bar in the picture indicated 0.5mm.

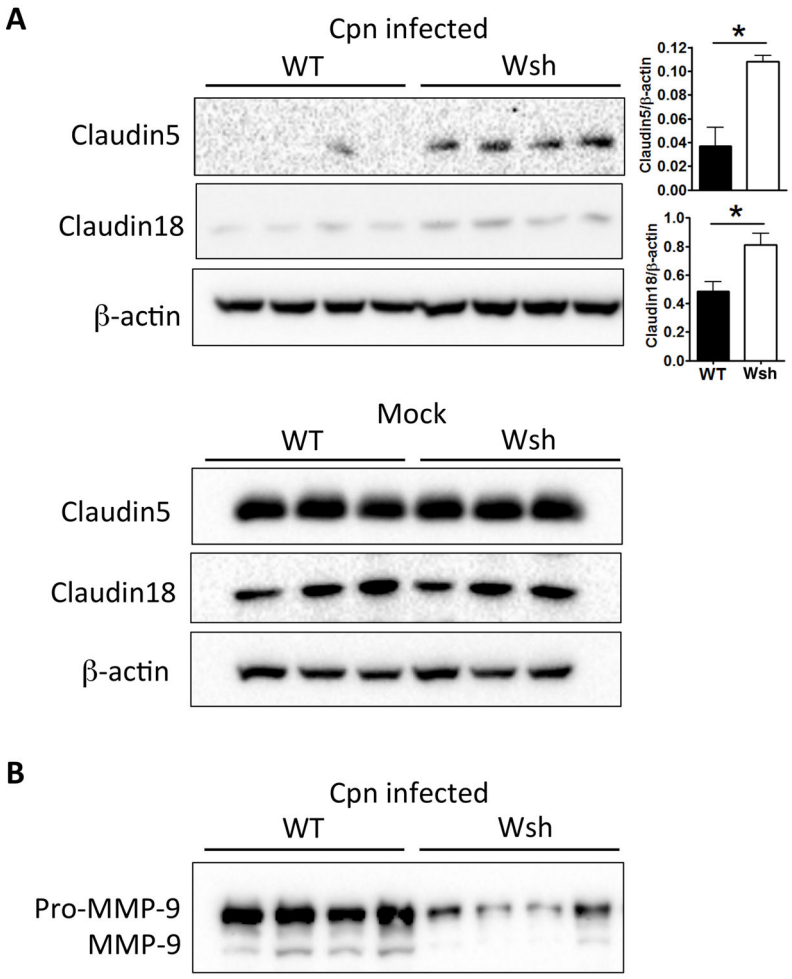

Figure 7. Cell-cell tight junction molecule degradation was reduced in Wsh lung compared to WT during Cpn lung infection

WT and Wsh mice were infected with 2×10^6 IFU Cpn intratracheally and sacrificed on day 5. (A) Lung cell lysates were separated by SDS-PAGE and immunoblotting was performed with indicated antibodies. The representative westerns are shown to analyze relative amounts of claudin 5 and 18 in the lung from naïve and Cpn-infected WT and Wsh mice. (B) BALF was separated by SDS-PAGE and immunoblotting was performed with anti-MMP-9 Ab to determined secreted MMP-9 in BALF. For A, this experiment was performed 3 times n=5 (WT) n=6 (Wsh). For A & B, the experiment was performed twice n=4 (WT) n=4 (Wsh). Data shown is a representative experiment. Data are mean ±SD. Significance of differences was determined by Mann-Whitney. *P<0.05.

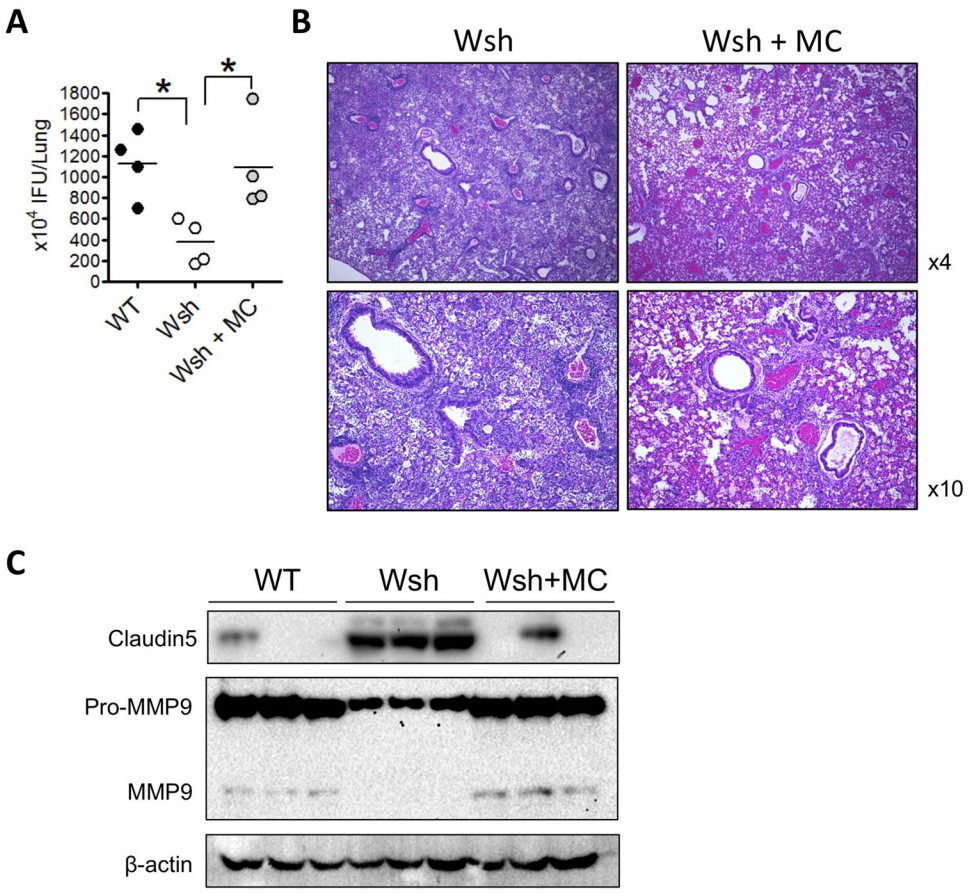

Figure 8. Mast cell reconstitution in Wsh mice restores normal responses to *C. pneumonia* infection

(A–C). Wsh mice were given 5×10^6 of MCs i.v. and allowed to reconstitute for 12 weeks. The mice were then infected with Cpn and sacrificed 5 days later. (A) Lung Cpn IFU was quantified at day 5 post infection. (B) H&E staining. (C) Western analysis of claudin 5 and MMP9 in the lung. Data are mean ±SD. Significance was determined using one-way ANOVA and Tukeys post hoc test. *P<0.05.